Theory of Polymer Brushes of Liquid-Crystalline Polymers

Victor M. Amoskov and Tatiana M. Birshtein*

Institute of Macromolecular Compounds, Academy of Sciences of Russia, 31 Bolshoy pr., 199004 St. Petersburg, Russia

Victor A. Pryamitsyn

Institute of Problems of Mechanical Engineering, Academy of Sciences of Russia, 61 Bolshoy pr., 199004 St. Petersburg, Russia

Received February 26, 1996; Revised Manuscript Received June 24, 1996[⊗]

ABSTRACT: Liquid crystalline ordering in polymer brushes formed by macromolecules with mesogenic groups in the main chain and immersed in a solvent is investigated theoretically by numerical calculations within a self-consistent field approximation. Existence of a microphase-segregated brush regime with a collapsed orientationally ordered intrinsic sublayer and a swollen external sublayer is shown. At high grafting density (σ), the transition from a conventional brush state to the microphase-segregated state is continuous. At small σ, it is a jumpwise first-order phase transition for a finite chain length (N), the magnitudes of the jumps in the average characteristics of the brush tend to zero in the limit $N \to \infty$.

1. Introduction

Theoretical and experimental studies of polymer brushes have been a very popular field of investigation for the last 10 years.[1−11] Advances in statistical theory, simulations, and experimental studies have made it possible to understand the behavior of polymer brushes in some detail. Nevertheless, they continue to be an inexhaustible object of investigation. This paper is devoted to a theoretical study of liquid-crystalline (LC) ordering in planar polymer brushes formed by macromolecules with mesogenic groups in the main chains and immersed in a solvent. We know only a few papers on LC transitions in polymer brushes. Reference 12 deals with the LC thermotropic transition in dry brushes. LC ordering in swollen brushes was investigated in refs 13 and 14; the case of grafted chains containing rigid segments and capable of lyotropic LC ordering with increasing concentration was considered there. It was shown that the brush behavior differs completely from that of free chains in solution. The chains in a brush are stretched, and an increase in polymer concentration in a brush (i.e. an increase in the grafting density) leads to a simultaneous increase in both the chain extension and the orientational segment order. As a result, the equilibrium state changes continuously without the phase transition typical of solutions. In ref 15 the case of the swollen brush with thermotropic mesogenic groups in polymer chains was considered by using a simple DeGennes−Alexander model[1−3] which is based on the hypothesis that all the chains have the same height of the free end. In this model the LC ordering of the brush occurs either as a discontinuous first-order phase transition which is similar (or even identical) to the transition in a polymer solution or, alternatively, as a continuous cooperative transition, depending on the grafting density of the brush.

To improve this model, we generalized the Scheutjens−Fleer self-consistent field theory of polymer systems[4] to analyze the details of the structure and thermodynamic properties of LC brushes.

[⊗] Abstract published in *Advance ACS Abstracts,* September 1, 1996.

2. Model

The main assumption of the molecular field approach to a heterogeneous system is to consider the free energy of a system as a function of local density and split it into two parts: the entropy of a system of noninteracting chains with the same density profile and the energy (more exactly the free energy) of short-range interactions calculated in the approximation of local homogeneity of the system. We calculate the entropy as the entropy of the system of noninteracting chains in an external field which forms the ordered structure. The entropy of a system in an external field $U(q)$ that is a function of the generalized coordinate q is

$$S[U] = \int U(q)\frac{\delta F[U]}{\delta U(q)}\,\mathrm{d}q - F[U] \tag{1}$$

where $F[U]$ is the free energy of the system and

$$\frac{\delta F[U]}{\delta U(q)} = \rho(q) \tag{2}$$

is the generalized density of the system.

The free energy of the system in the molecular field approach is

$$F_{\mathrm{mf}}[\rho] = \int f_{\mathrm{int}}[\rho(q)]\,\mathrm{d}q - S(U[\rho]) \tag{3}$$

where f_{int} is the density of the free energy of short-range interactions in the approximation of local homogeneity of the system, $U\{\rho\}$ is defined by inverting eq 2. Minimization of eq 3 with respect to ρ gives

$$U[\rho] = \frac{\delta f_{\mathrm{int}}[\rho]}{\delta \rho(q)} \tag{4}$$

The right part of eq 4 is the local exchange chemical potential of the system. Equations 2 and 4 form the complete set for calculation of ρ and U, usually called the self-consistent field equations.

2.1. Polymer Brush in an Anisotropic Field. Let us consider a simple cubic lattice model of polymer chains grafted to a flat surface in the external anisotropic field $U_i(x)$ (below we will use the function $\lambda^i(x) = \exp[-U_i(x)]$), where the x direction is perpendicular to

S0024-9297(96)00314-2 CCC: $12.00

the grafting surface and kT is used as an energy unit. The polymer chain is a sequence of oriented joined polymer segments. The directions of orientation are described and indexed as

$\odot$ — x direction

$+$ — four directions perpendicular to x

$\otimes$ — opposite to x

Let us introduce the partition function $P_N\binom{i\,j}{x\,y}$ of a polymer chain of N segments started from the layer x in the direction i and finished in the layer y with the direction j. Two different forms of recurrent relations of $P_N\binom{i\,j}{x\,y}$ correspond to adding a chain link to the beginning of the chain or to its end:

$$\begin{pmatrix} P_{N+1}\binom{\odot\quad j}{x-1\quad y} \\ P_{N+1}\binom{+\quad j}{x\quad y} \\ P_{N+1}\binom{\otimes\quad j}{x+1\quad y} \end{pmatrix} = \mathbf{A}\cdot(\Lambda[x])\cdot \begin{pmatrix} P_N\binom{\odot\quad j}{x\quad y} \\ P_N\binom{+\quad j}{x\quad y} \\ P_N\binom{\otimes\quad j}{x\quad y} \end{pmatrix} \tag{5}$$

$$\begin{pmatrix} P_{N+1}\binom{i\quad \odot}{x\quad y} \\ P_{N+1}\binom{i\quad +}{x\quad y} \\ P_{N+1}\binom{i\quad \otimes}{x\quad y} \end{pmatrix} = (\Lambda[y])\cdot\mathbf{A}^{\mathrm{T}}\cdot \begin{pmatrix} P_N\binom{i\quad \odot}{x\quad y-1} \\ P_N\binom{i\quad +}{x\quad y} \\ P_N\binom{i\quad \otimes}{x\quad y+1} \end{pmatrix} \tag{6}$$

where

$$\Lambda_{ij} = \begin{pmatrix} \lambda^{\odot}(x) & 0 & 0 \\ 0 & \lambda^{+}(x) & 0 \\ 0 & 0 & \lambda^{\otimes}(x) \end{pmatrix} \quad \text{and}$$

$$\mathbf{A}_{ij} = \begin{pmatrix} \alpha_t & 4\alpha_g & \alpha_b \\ \alpha_g & \alpha_t + 2\alpha_g + \alpha_b & \alpha_g \\ \alpha_b & 4\alpha_g & \alpha_t \end{pmatrix}$$

are the field and conformational propagation matrices ($\lambda^i(x) = 0$ if $x < 0$), α_t, α_g, and α_b are the statistical weights of direct (*trans* isomer), turn (*gauche* isomer), and back walks of the chain on the cubic lattice and $\mathbf{A}^{\mathrm{T}}$ is transposed to the $\mathbf{A}$ matrix.

The boundary condition for $N = 0$ is

$$P_0\binom{i\quad j}{x\quad y} = D_i\delta_{ij}\delta_{xy} \tag{7}$$

where

$$D = \begin{pmatrix} 1 \\ 4 \\ 1 \end{pmatrix}$$

Let us consider an assembly of chains of N segments grafted to the surface with surface density σ. The ith component of average density in the layer x is

$$\rho_N\binom{i}{x} \equiv \rho^i(x) = -\sigma\frac{\delta \log Z}{\delta U_i(x)} = \sigma\frac{\sum_{n=0}^{N} R_n\binom{i}{x}B_{N-n}\binom{i}{x}}{D_i\sum_{j,y} R_n\binom{j}{y}} \tag{8}$$

where

$$R_n\binom{j}{y} = \sum_i P_n\binom{i\quad j}{0\quad y}, \qquad R_0\binom{j}{y} = D_j\delta_{0y} \tag{9}$$

$$B_n\binom{i}{x} = \sum_{j,y} P_n\binom{i\quad j}{x\quad y}, B_0\binom{i}{x} = D_i \tag{10}$$

and

$$Z = Z[\lambda^{\odot}(x),\lambda^{+}(x),\lambda^{\otimes}(x)] = \sum_{j,y} R_n\binom{j}{y}$$

is the partition function of a chain in the brush.

The recurrent equations for $R_n\binom{j}{y}$ can be obtained from (6) and for $B_n\binom{i}{x}$ from (5). The entropy per unit area of the brush in the external field $U_i(x)$ is

$$S_b[U] = \sigma \ln Z + \sum_{i,x}\{U_i(x)\rho^i(x)\} \tag{11}$$

This entropy can be interpreted as the entropy $S[U(\rho^i(x))]$ of the formation of a brush with the anisotropic density profile $\rho^i(x) \equiv \rho_N\binom{i}{x}$, where field $U[\rho]$ is calculated by inverting eq 8.

The free end distribution function $g[x]$ is

$$g[x] = N\frac{\sum_{i=1}^{3} R_N\binom{i}{x}}{\sum_{i,x} R_N\binom{i}{x}} \tag{12}$$

The total average local density in the layer x is

$$\rho[x] = \rho_N\binom{\odot}{x} + \rho_N\binom{+}{x} + \rho_N\binom{\otimes}{x} \tag{13}$$

The local degree of stretching $s_1[x]$ is

$$s_1[x] = \frac{\rho_N\binom{\odot}{x} - \rho_N\binom{\otimes}{x}}{\rho[x]} \tag{14}$$

The local orientational order parameter $s_2[x]$ is

$$s_2[x] = \frac{3}{2}\left(\frac{\rho_N\binom{\odot}{x} + \rho_N\binom{\otimes}{x}}{\rho[x]}\right) - \frac{1}{2} \tag{15}$$

The average value $\langle f[x]\rangle$ of an arbitrary function of x is

$$\langle f[x]\rangle = \frac{\sum_x f[x]\rho[x]}{\sum_x \rho[x]} \tag{16}$$

2.2. Molecular Field Approach to the Anisotropic Brush. For the calculation of f_{int} we suggest a combination of the Flory–Huggins model for the isotropic part (including excluded volume effects)[16,17] and the Maier–Saupe expression for the anisotropic interaction:[15]

$$f_{\mathrm{int}}[x] = (1 - \rho[x])\ln(1 - \rho[x]) - \chi\rho^2[x] - \frac{\eta}{2}\rho^2[x]s_2{}^2[x] \tag{17}$$

where χ and η are the parameters of isotropic and anisotropic interactions between polymer segments, all

the terms linear in ρ are ignored, because they do not affect the results (in the case of purely isotropic interaction, $\eta = 0$ and χ is the conventional Flory parameter χ). The free energy per unit area of the brush is

$$F_b = \sum_x f_{int}[\rho(x)] - S_b[U(\rho)] \tag{18}$$

The minimization of F_b gives us the equation for the self-consistent potential $U_i(x) = -\log \lambda^i(x)$:

$$\left.\begin{aligned} \lambda^{\odot}(x)=\lambda^{\otimes}(x)=(1-\rho[x])\exp\{\rho[x](2\chi+\eta s_2[x])\} \\ \lambda^{+}(x)=(1-\rho[x])\exp\left\{\rho[x]\left(2\chi-\frac{\eta}{2}s_2[x]\right)\right\} \end{aligned}\right\} \tag{19}$$

These equations mean that the profile of the local chemical potential of polymer segments $\partial f_{int}/\partial\rho$ needs to be equal to the potential of the field forming the density profile $\rho^i(x)$. The formulas 8 and 19 form a set of equations of self-consistent field (SCF) theory for calculating $\lambda^i(x)$ and $\rho^i(x)$. This set has been solved numerically by the iteration method.

3. Results and Discussion

3.1. Structure of Brushes. We investigate the dependence of the structure of brushes on the magnitude of the anisotropic interaction parameter η. The brushes are formed by chains represented by walks on a simple cubic lattice. We vary the following parameters: chain length (N), statistical weights of isomers (α_t, α_g, α_b), grafting density (σ), and isotropic interaction parameter (χ). The requisite computer memory and the requisite processor time for one iteration grow approximately as $\sim N^2$ with increasing N. Moreover, the requisite number of iterations, which would have secured the necessary accuracy, is increasing approximately proportional to N with increasing N. Due to these reasons only systems with $N \leq 500$ were investigated.

The brush structure is characterized by the distributions of segment density ρ, order parameter s_2, and free ends g inside the brush.

The typical examples of the results of our calculations are shown in Figures 1a−c and 2a−c. One can see three possible regimes of brush behavior, which we designate as conventional brush (CB), liquid-crystalline brush (LCB), and microphase-segregated brush (MSB) regimes.

The CB regime is realized at small η, i.e. $\eta < \eta_1$, where η_1 is a function of grafting density σ and isotropic interaction parameter χ (it increases with a decrease in σ and χ). In this regime the density profile and free end distribution are practically independent of η and coincide with the well-known dependence for brushes with only isotropic interactions between segments ($\eta = 0$).[6,7] The η value influences the profile of the order parameter, but nevertheless this order parameter is not very large.

The LCB regime is realized at sufficiently large η, i.e. at $\eta > \eta_2$, where $\eta_2 > \eta_1$ is also the function of σ and χ and increases with a decrease in σ and χ. In this regime we have a steplike dense brush ($\rho \simeq 1$) with a high degree of orientational order of the segments ($s_2 \simeq 1$). This LCB state corresponds to the LC state in the steplike brush model.[15] However, unlike the approximation on the steplike model, the free ends of chains are distributed in the brush (Figures 1c and 2c). The form of distribution corresponds to that for the collapsed brush in a poor solvent.[6] In both cases the maximum distribution is located near the upper boundary of a brush.

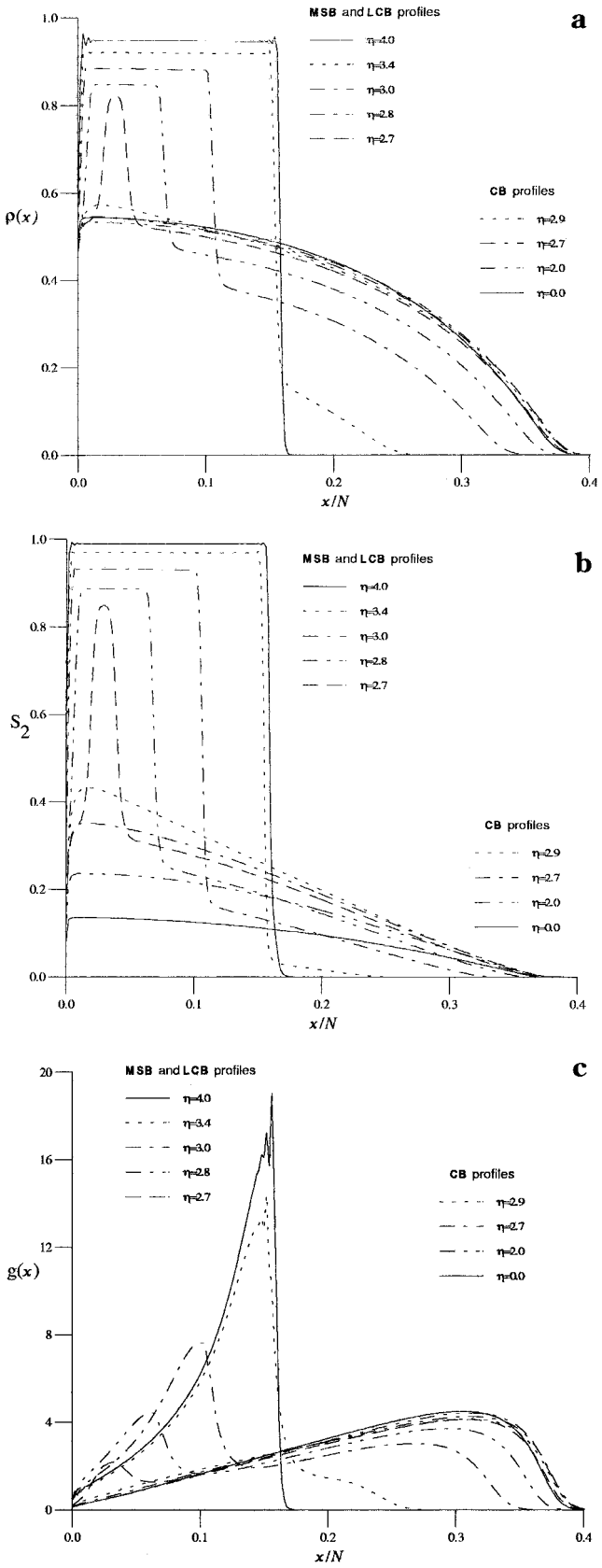

Figure 1. Profiles of brush characteristics at different energies η of the anisotropic interaction (given in the figures): (a) density profiles $\rho(x)$; (b) profiles of the orientational order parameter $s_2(x)$; (c) free end distributions $g(x)$. $\sigma = 0.15$; $N = 500$; $\chi = 0.25$; 6-choice SCL.

The MSB regime, located between the two limiting CB and LCB regimes, $\eta_1 < \eta < \eta_2$, seems to be of

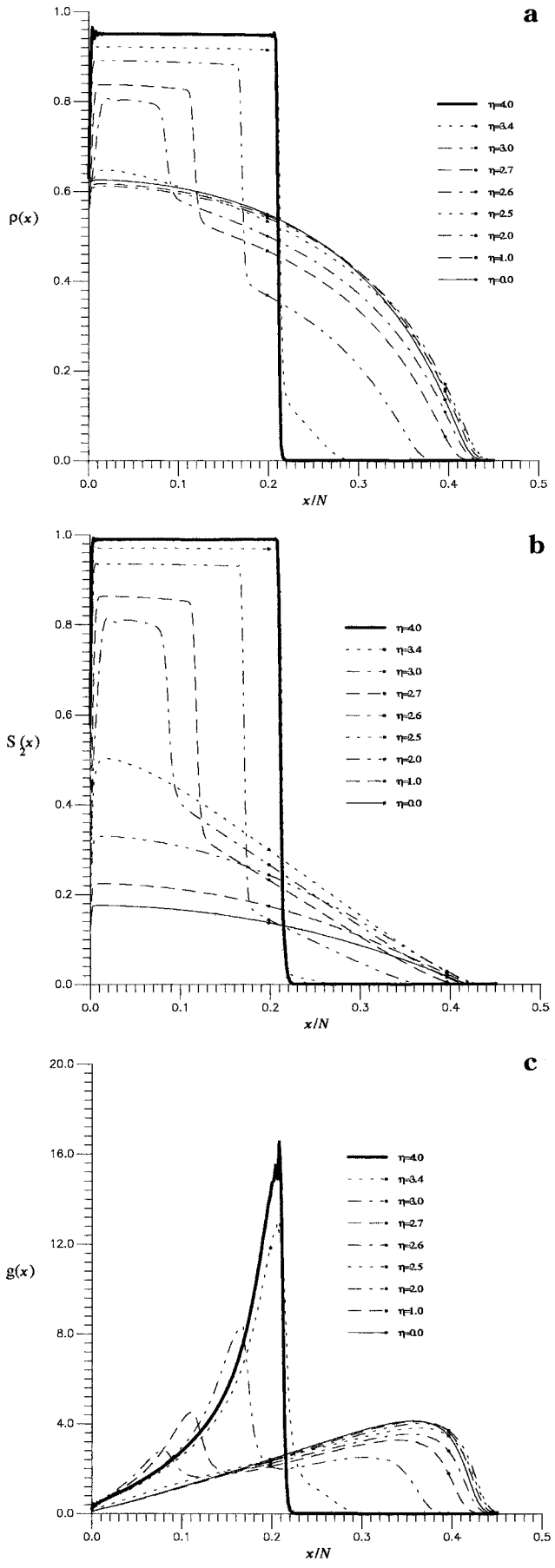

Figure 2. Profiles of brush characteristics at different energies η of the anisotropic interaction (given in the figures): (a) density profiles $\rho(x)$; (b) profiles of the orientational order parameter $s_2(x)$; (c) free end distributions $g(x)$. $\sigma = 0.25$; $N = 500$; $\chi = 0.25$; 6-choice SCL.

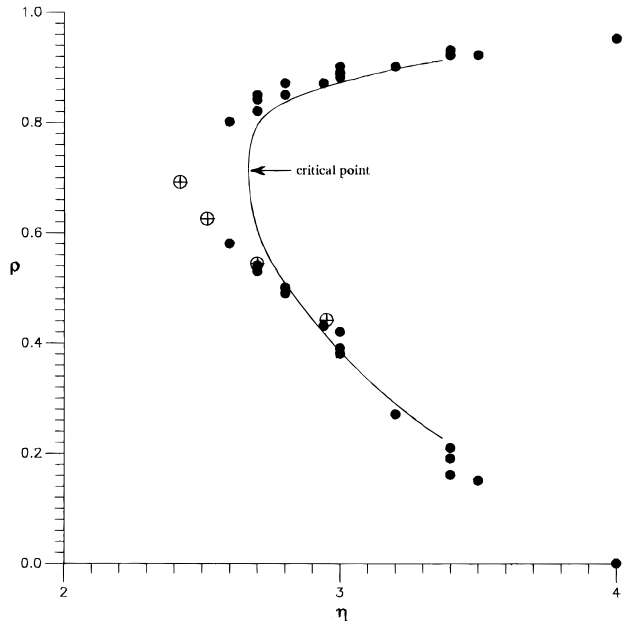

Figure 3. Phase diagram for the brushes in the box-model approximation[15] (solid line, the position of the critical point is shown by the arrow) and data from the present work: (●) intrinsic boundaries in brushes in the MSB regime; (⊕) maximal density in the brush at $\eta = 0$ versus the transition energy η_t. $N = 500$; $\chi = 0.25$; 6-choice SCL.

particular interest. Two limiting structures are combined in the same brush in this regime: the LCB structure in the intrinsic part of the brush near the grafting surface and the CB structure at the periphery. The boundary between these two structures inside the brush is very well pronounced by the abrupt jumps in density and order parameter (Figures 1a,b and 2a,b). The free end distribution in this regime is bimodal (Figures 1c and 2c). The first maximum corresponds to the one in the LCB regime and is located in the intrinsic LCB layer near the upper boundary of this layer (the boundary between two structures). The form of the second maximum, placed in the external CB layer, corresponds to the form of free end distribution in the CB regime. These results give an indication that the two states inside the brush are two different phases, divided by the interface boundary. In other words, in the MSB regime we have microphase segregation inside the brush.

3.2. Microphase Segregation inside the Brush. To gain a better insight into the nature of microphase segregation inside the brush, let us compare our results with those for the simple boxlike model of the brush.[15] It was shown in ref 15 that for this simple model the increase in the anisotropic interaction parameter η leads to the first-order phase transition from the conventional swollen state to a collapsed strongly oriented state, i.e. to the CB → LCB transition. Figure 3 represents the binodal for this transition in (η,ρ) coordinates. The lower branch of the binodal corresponds to the CB regime; the upper branch, to LCB regime. Note that the segment density ρ is not the arbitrarily assigned quantity in a brush. It is a function of grafting density σ, and in the box model we have for the CB regime:

$$\rho = K\sigma^{\nu} \tag{20}$$

where $\nu = {}^2/_3$ and ${}^1/_2$ for the good and Θ-solvent conditions, correspondingly, and K is a coefficient of the order of unity, depending on χ under good-solvent conditions. Hence each pair of points on the binodal at

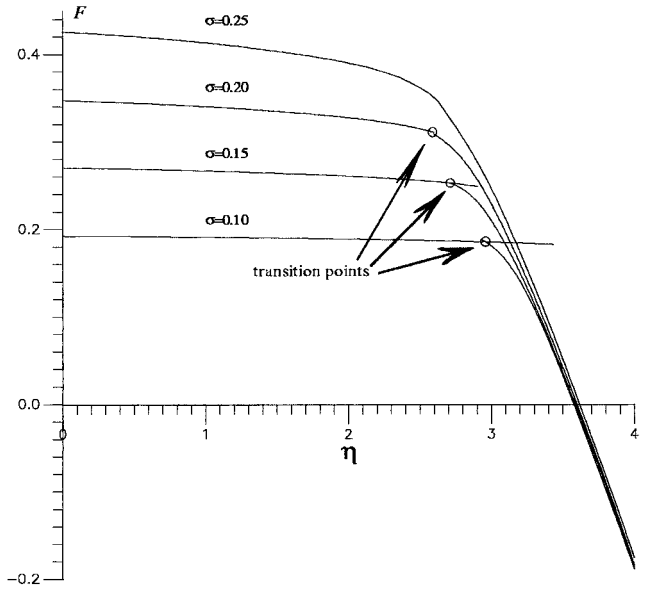

Figure 4. Free energy per segment in the brush versus the energy η of the anisotropic interaction for different grafting densities $\sigma = 0.10, 0.15, 0.20, 0.25$ (numbers on the curves). $N = 500$; $\chi = 0.25$; 6-choice SCL.

the same η (one on the lower and the other on the upper branch) corresponds to its own value of σ, increasing from the right to the left up to the critical point. At $\chi = 0.25$ the critical values of parameters are $\sigma_{cr} \simeq 0.2$, $\rho_{cr} \simeq 0.76$, and $\eta_{cr} \simeq 2.6$ (see Figure 3). At a larger grafting density the LC ordering of the brush in this model is not a first-order phase transition but proceeds smoothly with the increase in anisotropic interaction η.

In our system, each value of σ is related not just to a pair of points on the phase separation curve, but rather to a pair of continuous sets of points. In fact, within the interval of $\eta_1 < \eta < \eta_2$, where the MSB regime is found, the brush combines both phases (LCB in the inner part of the brush and CB in the outer part) separated by a boundary.

The dependences $\rho^* = \rho^*(\eta)$ and $\rho^{**} = \rho^{**}(\eta)$ of the segment densities on the outer boundary of the intrinsic LCB state and inner boundary of the external CB state (see Figures 1a−c and 2a−c) are also plotted in Figure 3. It is easy to see that all the data for different σ fall into branches of the binodal for a boxlike model: ρ^* values are located near the upper branch; ρ^{**}, near the lower branch.

Hence, the microphase separation inside the brush with inhomogeneous distribution of density is at least in a first approximation similar to the phase transition in a box model. The jumps in density and degree of order inside the brush substitute for the jumps in these characteristics for a brush as a whole in a boxlike model.

3.3. Phase Transition CB → MSB. Let us now consider the brush behavior near the MSB/LCB and CB/MSB boundaries: $\eta = \eta_2$ and $\eta = \eta_1$. From Figures 1a−c and 2a−c it follows that both the density and the width of the intrinsic LC layer in the MSB regime are increasing functions of η. At $\eta = \eta_2$ this layer extends over the total height of the brush.

The transition from the CB regime to the MSB regime at $\eta = \eta_1$ has some peculiarities. As one can see from Figure 1a−c, in the case of small grafting density $\sigma = 0.10, 0.15$, the results of calculations are ambiguous in a small interval of the η values near $\eta = \eta_1$. Using different structures as an initial guess of iterations in this interval of η, it is possible to find two different solutions of SCF equations, which correspond to the CB and MSB regimes (Figure 1a−c). One of these solutions is the global minimum of free energy corresponding to the stable state of the brush; the other is the local minimum corresponding to the metastable state. Note that at larger grafting density ($\sigma \geq 0.2$) the conversion from CB to MSB is continuous (Figure 2a−c).

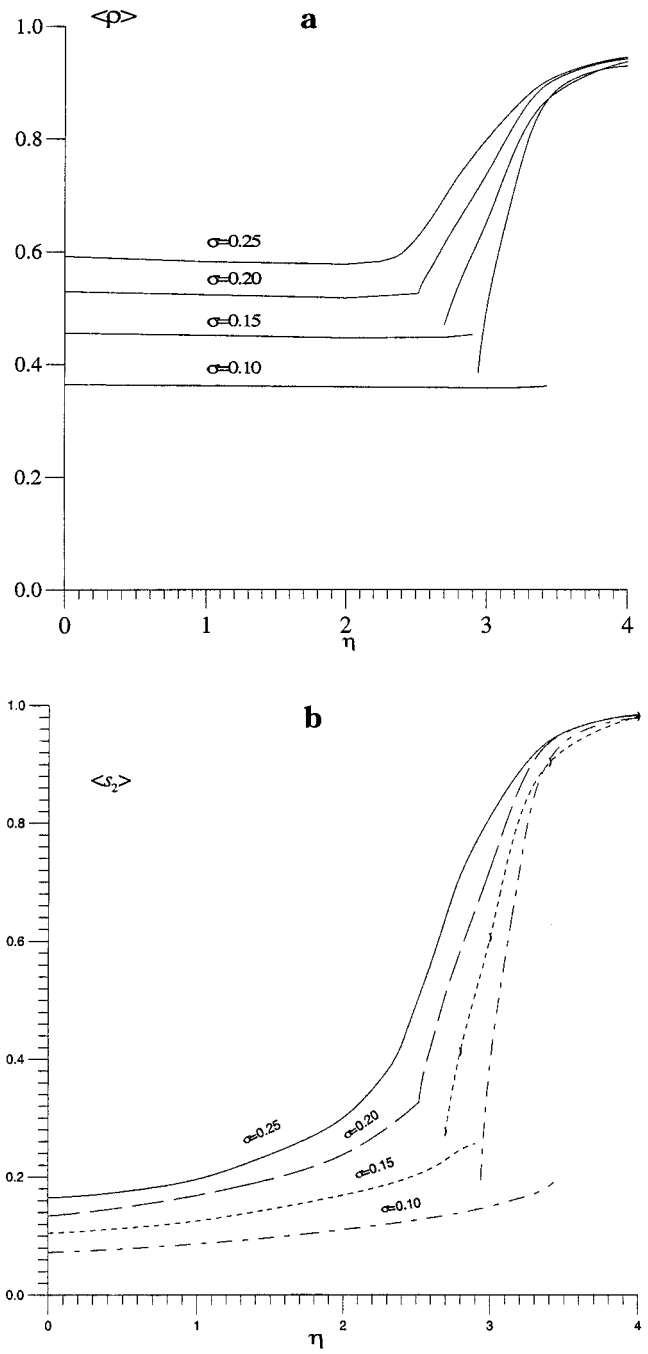

Figure 5. Average characteristics of the brush: segment density $\langle\rho\rangle$ (a) and order parameter $\langle s_2\rangle$ (b) versus η at different $\sigma = 0.10, 0.15, 0.20, 0.25$ (numbers on the curves). $N = 500$; $\chi = 0.25$; 6-choice SCL.

To discriminate between stable and metastable states, we have investigated the free energies of these states. The dependence of $F = F(\eta)$ is presented in Figure 4 for four values of grafting density σ. It is easy to see that the dependence $F = F(\eta)$ breaks into two branches. Moreover, these branches intersect each other in the case of low grafting density ($\sigma = 0.10, 0.15$). The intersection of two branches of free energy is an evidence of the first-order phase transition occurring at the point $\eta = \eta_t$, where η_t is the intersection point. At $\eta < \eta_t$ the brush in equilibrium is in the CB regime.

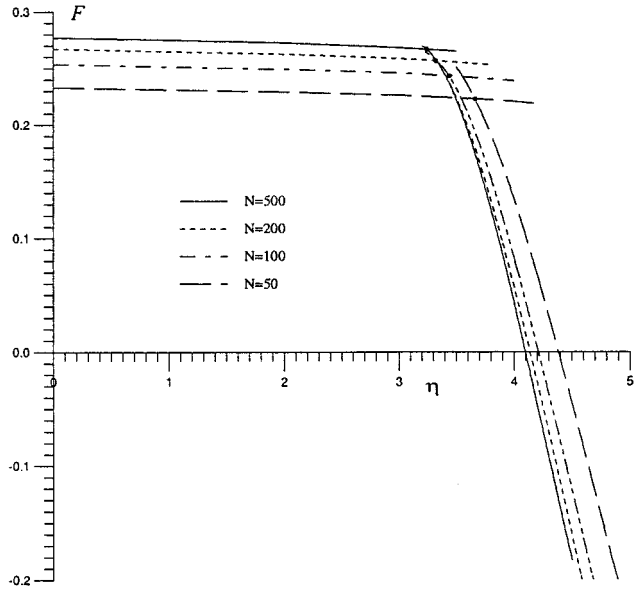

Figure 6. Free energy per segment in a brush versus the energy η of the anisotropic interaction for chains with different N ($\sigma = 0.10$; $\chi = 0$; 6-choice SCL). The dependences are shifted along the y-axis according to each other.

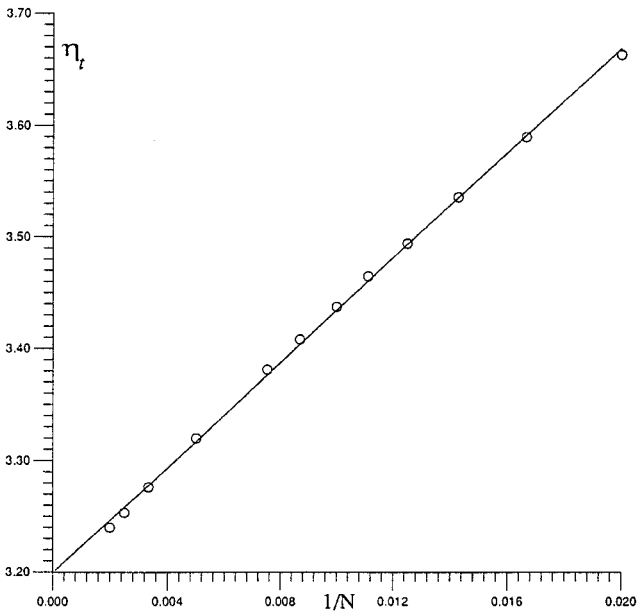

Figure 7. Molecular weight dependence of transition point η_t in the brush. $\sigma = 0.10$; $\chi = 0$; 6-choice SCL.

The free energy in this regime is independent of η and is the function of grafting density only. At $\eta > \eta_t$ the equilibrium corresponds to the MSB regime. On the subsequent increase of η the system transfers into the LCB regime, where the free energy is independent of σ and is a linear function of η (due to the third term in the right side of eq 17). Near the transition point η_t there is a range of η where we observe not only stable but also metastable structures: the MSB structure within a narrow interval of η at $\eta < \eta_t$ and the CB structure in broader interval at $\eta > \eta_t$. The existence of metastable states is also a characteristic property of the first-order phase transition (such as effects of supercooling).

A sharp transition from the CB to the MSB regime at low grafting density is manifested in the dependence of the average characteristics of brushes on η. Figure 5 shows the mean segment density (Figure 5a) and the mean parameter of orientational order (Figure 5b) as a function of energy of anisotropic interaction η at different grafting densities. At low grafting density ($\sigma = 0.10-0.15$) there are the marked differences in the slopes of functions $\langle\rho(\eta)\rangle$ and $\langle s_2(\eta)\rangle$ to the right and to the left of the transition point and a more or less pronounced jump in the transition point.

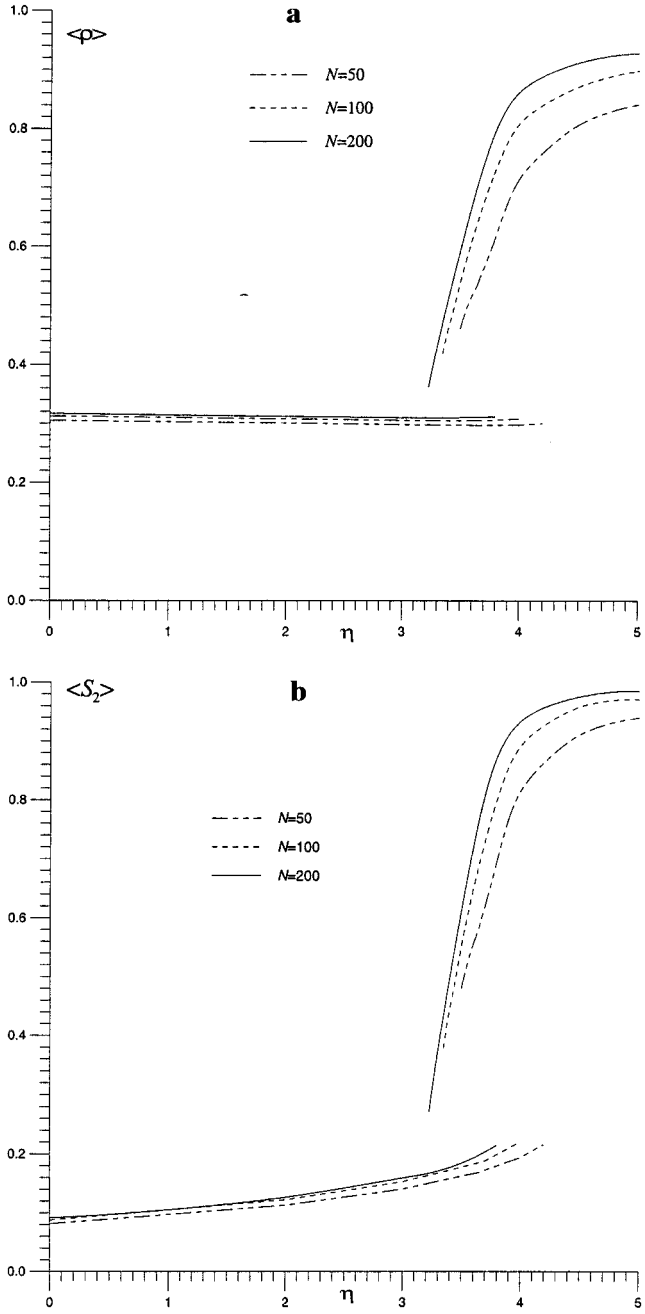

Figure 8. Average characteristics of the brush: segment density $\langle\rho\rangle$ (a) and order parameter $\langle s_2\rangle$ (b) versus η at different $N = 50-500$ (numbers on the curves). $\sigma = 0.10$; $\chi = 0$; 6-choice SCL.

The investigation of characteristics of brushes generated by chains of different lengths $N = 50, ..., 500$ shows that in the whole region of η (excluding small region near η_t) we obtain closely related results for different N, providing we use the reasonable coordinate x/N. The value of N, however, markedly affects both the position and peculiarties of transition CB/MSB. As can be seen from Figures 6 and 7 the position of transition point η_t is a linearly increasing function of $1/N$ (decreasing function of N). The increase in N also leads to the decrease of the jumps of average brush characteristics in transition from the CB to the MSB state (Figure 8).

The jumpwise change in the average characteristics of the brush as a whole, obtained for $N \leq 500$, seems to

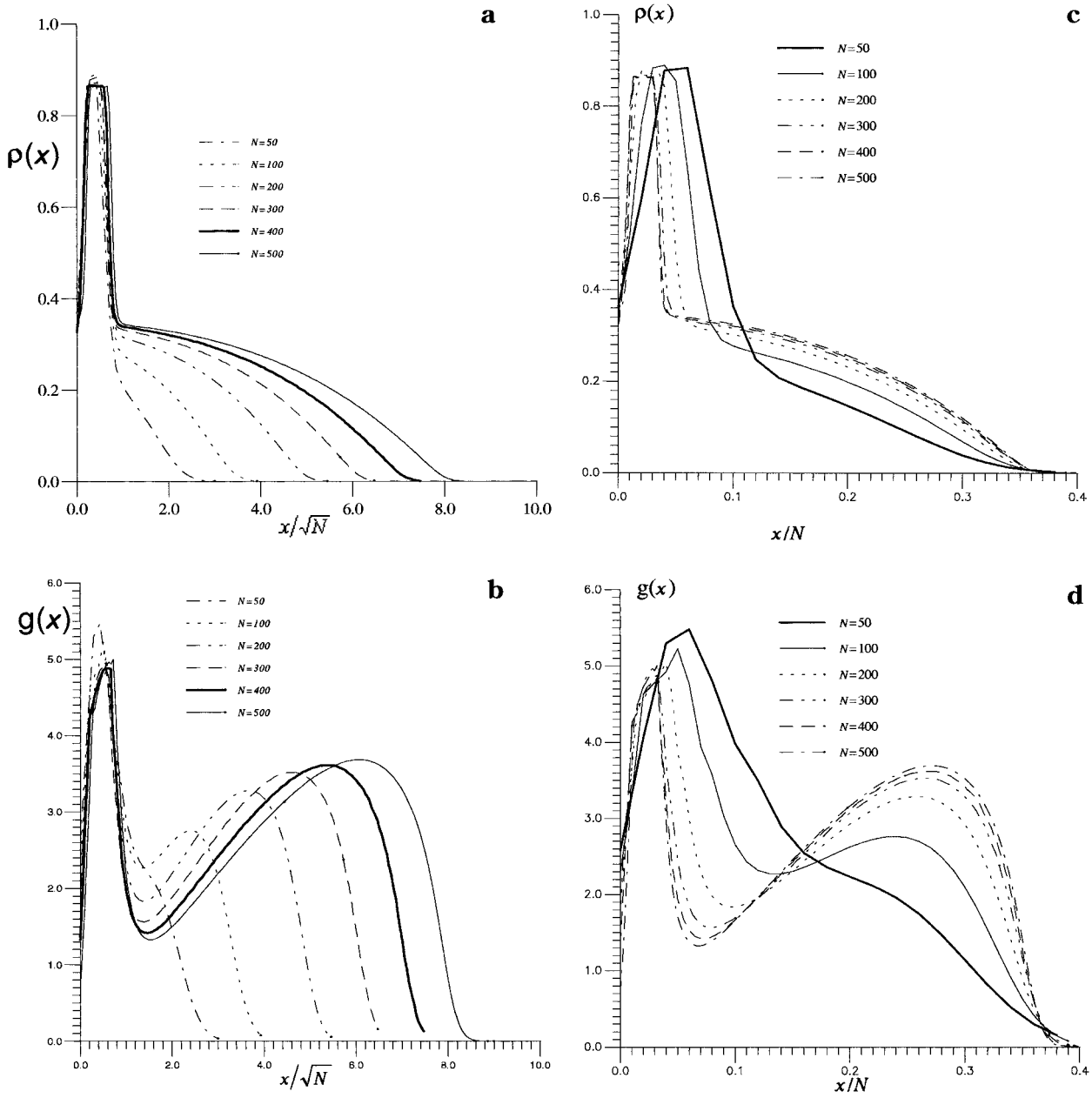

Figure 9. Profiles of brush characteristics at different N in the transition point $\eta_t(N)$ as functions of $x/\sqrt{N}$ (a, b) and x/N (c, d). Density profile $\rho(x)$ (a, c) and free end distribution $g(x)$ (b, d). $\sigma = 0.10$; $\chi = 0$; 6-choice SCL.

be a result of the finite chain length. The phase structure of the CB/MSB transition is conserved in the limit $N \to \infty$, but the magnitude of the jumps in average characteristics of the brush tends to zero since this transition occurs only in a vanishingly small part of the brush. This conclusion is confirmed by the molecular weight dependences of the thickness of the LCB sublayer arising at the point $\eta = \eta_t(N)$. As can be seen from Figure 9, this thickness scales as $N^{1/2}$, which is in contrast with the scaling law for the thickness of the layer as a whole ($\sim N$). (The thickness of the LCB sublayer in the MSB regime far from the transition point also scales as N.) Hence the contribution of the LCB sublayer to the average characteristics of the layer at the transition point is proportional to $N^{-1/2}$ and tends to zero at $N \to \infty$.

At larger grafting density $\sigma = 0.20$, 0.25 the CB/MSB transition has no jump of a similar nature at any N. The dependence $F = F(\eta)$ turns out to be smooth, but the second-order phase transition cannot be excluded. Note that in all these cases (both at small σ and at relatively large σ) there is a microphase segregation inside the layer.

3.4. Effect of the Flexibility of Grafted Chains. Thus far we investigated the LC transition only for the flexible chains on 6-choice SCL. Let us consider briefly the general trend in the dependence of the position of transition and conformations of chains on the condition of internal rotation. Figure 10 demonstrates the free energy, the average segment density, and the average order parameter versus η dependences for three lattice models:

(1) 6-choice SCL; $\alpha_t = \alpha_g = \alpha_b = 1$, model (111)

(2) 5-choice SCL: back-step is prohibited, the statistical weight of each *gauche* conformation is equal to the statistical weight of the *trans* conformation; $\alpha_t = \alpha_g = 1$, $\alpha_b = 0$, model (110)

(3) 5-choice SCL: back-step is prohibited, the statistical weight of the *trans* conformation is 4 times larger than the statistical weight of each *gauche* conformation; $\alpha_t = 4$, $\alpha_g = 1$, $\alpha_b = 0$, model (410).

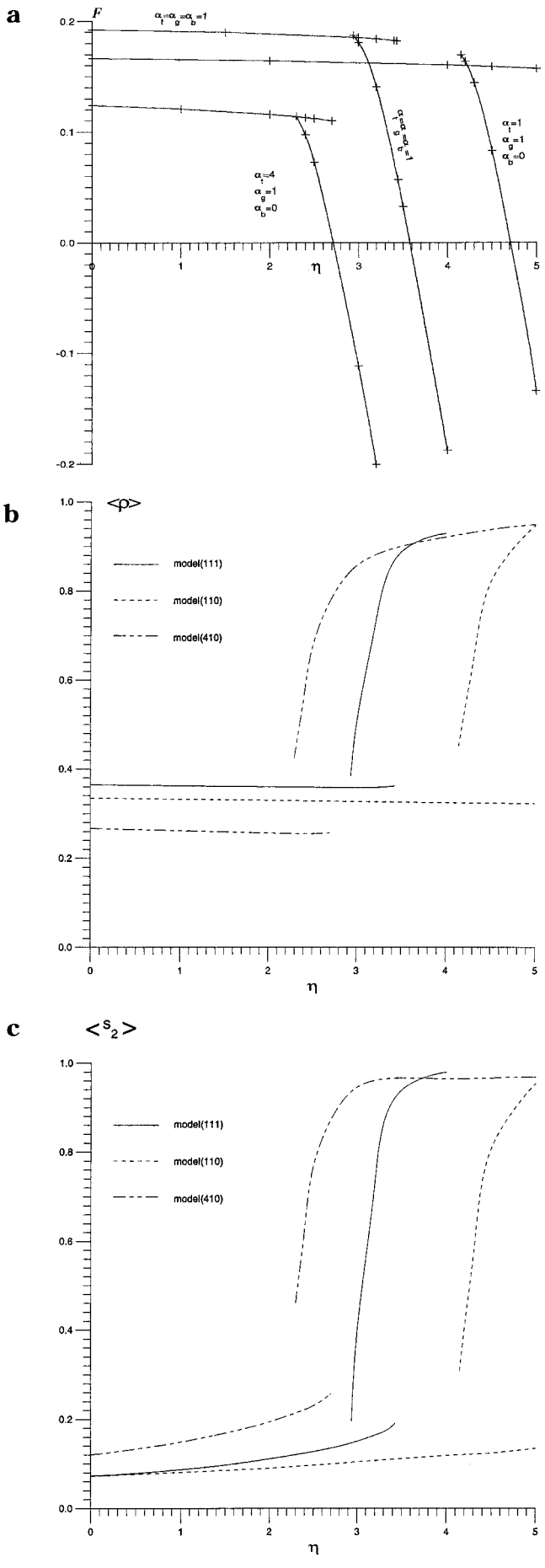

Figure 10. Free energy per segment (a), segment density $\langle\rho\rangle$ (b), and order parameter $\langle s_2\rangle$ (c) versus η for different models (see text). $\sigma = 0.10$; $\chi = 0.25$; $N = 500$.

In these models we have the monotonous decrease in flexibility in the sequence

$$(111) \rightarrow (110) \rightarrow (410)$$

The statistical (Kuhn) segments l in free Gaussian chains are equal to $l_1 = 1$, $l_2 = 1.5$, and $l_3 = 3$, respectively. At the same time, as can be seen from Figure 10a, the transition point η_t shifts to larger values of η on going from model (111) to model (110), and to a smaller value on going from models (111) and (110) to model (410). The decrease of η_t in the sequence (110) → (410) is easy to obtain with respect to the value of flexibility. The energy of the disorder−order transition must be sufficient to compensate for the loss of entropy due to ordering. For a given mechanism of flexibility it is possible to assume that the entropy loss related to the statistical segment is kept constant no matter how great the length of the segment may be. From this it follows:

$$\eta_t \sim 1/l \tag{21}$$

From Figure 10a it follows that $\eta_t(110)/\eta_t(410) = 4.2/2.3 \simeq 1.8$ in good agreement with the $l_3/l_2 = 2$ value.

The transfer from model (111) to model (110) as distinct from (110) → (410) transfer is due to the change of not only the value of flexibility but also the mechanism of flexibility. In the 6-choice SCL model this mechanism allows the direct change of chain direction by 180°; in the 5-choice models it restricts the value of angle between two successive steps. It is possible to relate the 6-choice and 5-choice SCL models to the chains with rotational isomeric and persistent mechanisms of flexibility. The difference in the local conformations of chains is especially important in the orientationally ordered LC state. In the limit $s_2 \rightarrow 1$, the chain units in the model (111) can move freely back and forth along the x-axis. The chain retains its flexibility and its minimal entropy per link is log 2. In the 5-choice model the ordered chain loses its flexibility: the length of statistical segment l is an infinitely increasing function of the degree of order s_2, and at $s_2 \rightarrow 1$ the entropy per link approaches zero. This larger entropy loss in the ordered state for model (110) as compared to model (111) is responsible for the result $\eta_t(110) > \eta_t(111)$ (Figure 10a−c).

As follows from the results obtained, the chains in the LC layer (in the LCB sublayer in the MSB regime or in a brush as a whole in the LCB regime) totally fill the layer ($\rho \simeq 1$). The flexibility of ordered chains markedly affects the mode of filling the layer. Consider the chains ending in the LCB layer (or sublayer). In contrast to flexible chains (model (111), 6-choice SCL) moving back and forth along the x-axis at each step, the chains with induced rigidity (models (110) and (410), 5-choice SCL) form long rigid segments packed in a folded structure inside the layer.

It is interesting that the difference in the conformations of the chain affects the form of the free end distribution function inside the LCB layer (sublayer). For flexible chains (model (111), 6-choice SCL) the distribution (Figures 1c and 2c) is similar to that of the CB collapsed in a poor solvent.[6] This distribution has one relatively broad maximum, located near the upper boundary of the layer/sublayer. Figures 11b and 12b show the free end distribution for 5-choice SCL models. It is easy to see that the form of distribution inside the LC layer/sublayer is more complicated than in the first case (Figures 1c and 2c). Instead of one broad maxi-

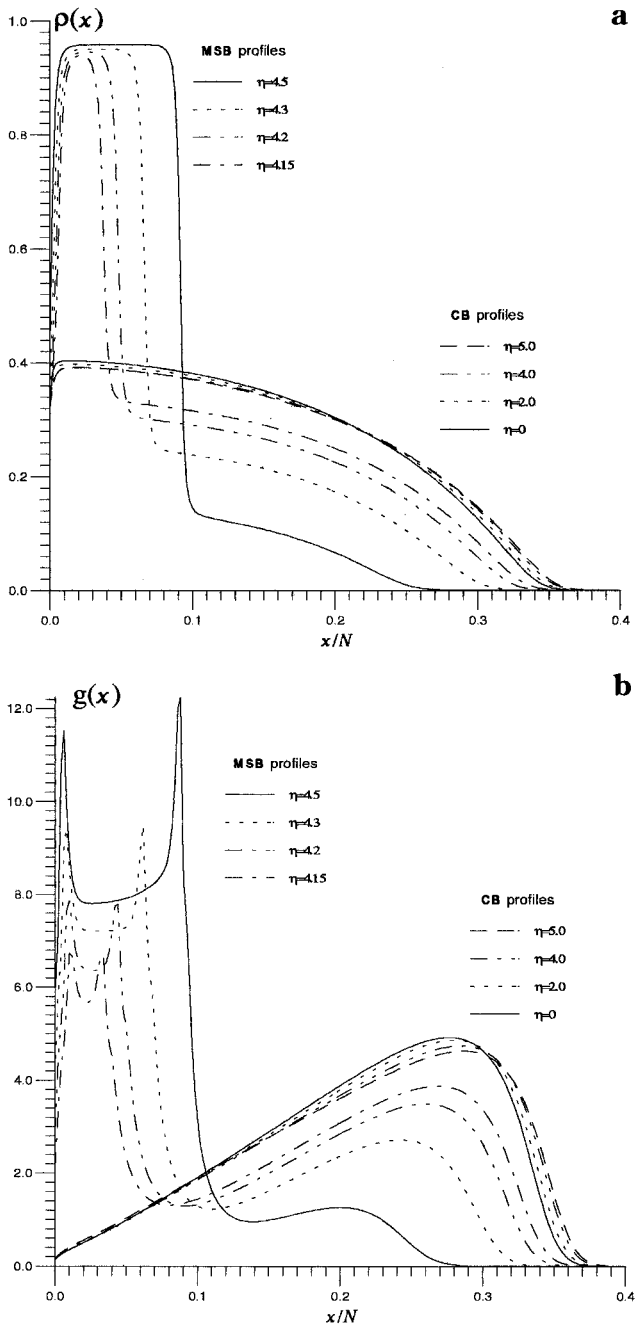

Figure 11. Density profiles $\rho(x)$ (a) and free end distribution $g(x)$ (b) in the brushes for the 5-choice SCL (110) model at different energies η of the anisotropic interaction (given in the figures). $\sigma = 0.10$; $\chi = 0.25$; $N = 500$.

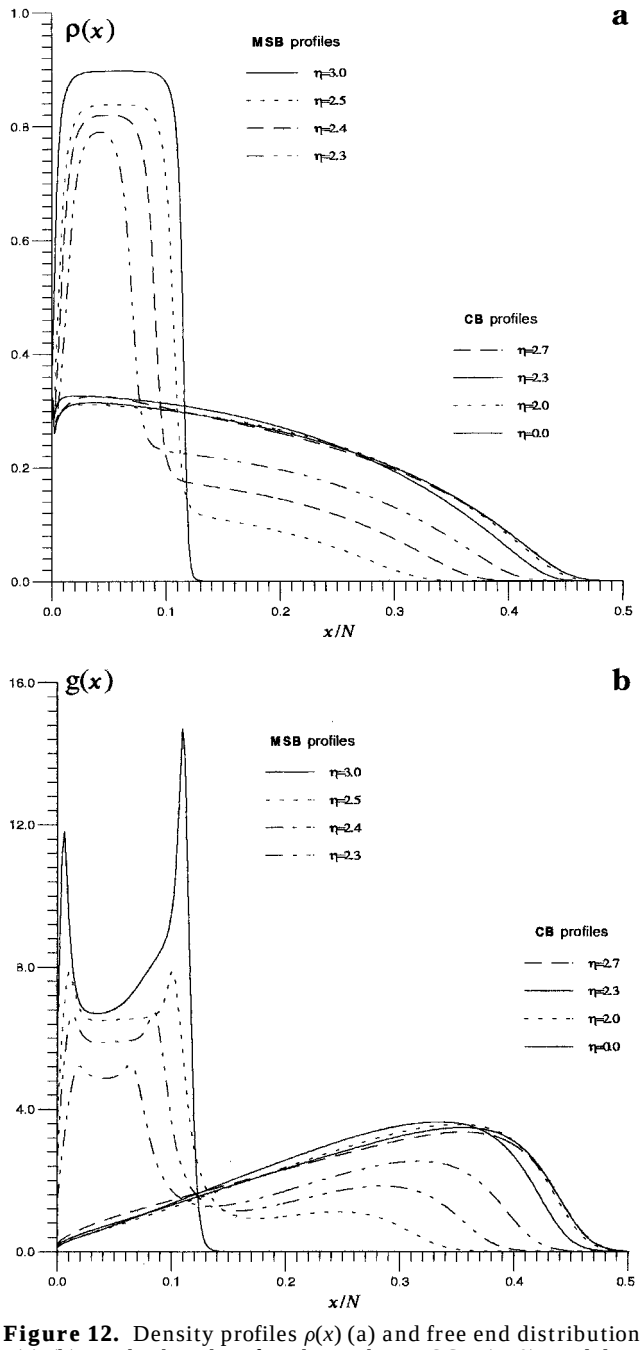

Figure 12. Density profiles $\rho(x)$ (a) and free end distribution $g(x)$ (b) in the brushes for the 5-choice SCL (410) model at different energies η of the anisotropic interaction (given in the figures). $\sigma = 0.10$; $\chi = 0.25$; $N = 500$.

mum one can see two maxima, located more or less symmetrically near the lower and upper boundaries in the regions of chain folding. Note that due to defects the decay of density on the extremes of the sublayer is not so abrupt for 5-choice models as for the 6-choice model (Figures 1a, 2a, 11a, and 12a). With sufficiently large η, when the total brush is in the LCB regime, the additional maximum of the free end distribution appears in the middle of the layer (Figure 13). Such a position is typical of a chain inside the flat slit, providing the thickness of the slit is larger than the Kuhn segment of the chain. In our case of chains with induced rigidity the nature of this maximum is not clear. Note also that odd−even oscillations in the curve for more rigid chain (model (410)) are the artifact of a lattice model.

3.5. Partial Characteristics of Chains. So far we have analyzed the characteristics of the total system of grafted chains as a whole. But the algorithm, considered in section 2.1, can be easily modified for the calculation of partial characteristics of chains in the brushes. To take an example, it is possible to consider the partial characteristics (density profile etc.) of a group of chains having their free ends within a given layer

$$x_1 \le x \le x_2$$

where x_1 and x_2 are arbitrary parameters.

Figure 14 shows some results of calculations. Two sets of data are presented in Figure 14 for two states of the brush equilibrated at $\eta = \eta_t$: the MSB state and the CB state. The partial characteristics are calculated for two groups of chains. Let l_t be the thickness of the LC layer in the MSB state. The chains with the position of ends $x \le l_t$ belong to the first group (finishing, or f-chains), and the chains traveling through this sublayer $x \ge l_t$ belong to the second group (t-chains).

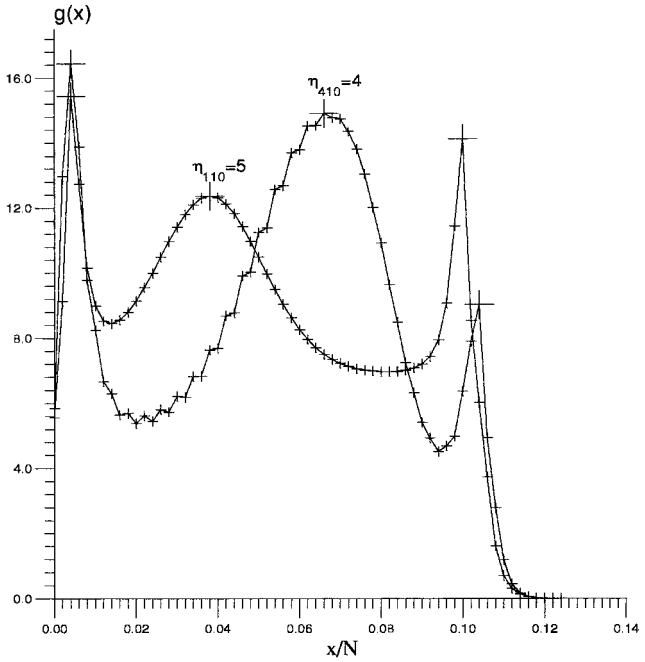

Figure 13. Free end distribution in the 5-choice SCL models at large energy η of the anisotropic interaction (numbers on the curves). $\sigma = 0.10$; $\chi = 0.25$; $N = 500$.

As follows from Figure 14a the density of f-chains in the MSB state is much higher than the density of f-chains in the CB state. The density profile of f-chains is more or less similar to the overall density profile in the MSB state. The density profile of t-chains has some peculiarities in the regions of the LC sublayer in the MSB state. In the middle part it is similar to the density profile of t-chains in the CB state, but there is the difference near the extremes of the LC layer, especially near the upper boundary of the LC layer. The density of t-chains in the MSB state has the well-pronounced maximum and minimum in this region.

The other peculiarities near the upper boundary of the LC layer in the MSB state are also shown in Figure 14b. This figure presents the partial degrees of stretching $s_1[x]$, see formula 14, for two groups of chains. It is interesting that in the middle part of the LC layer in the MSB state the profiles of the degree of stretching of both f- and t-chains are similar (for f-chain identical) to those in the CB state. Near the upper boundary of the LC layer there is the deep minima of the degree of stretching. For f-chains outside the layer $x < l_t$ the value of "stretching" becomes negative, which means that the number of back-steps is larger than the number of forward steps. This is possible only on the top of the loop.

The difference in conformations of chains in the (111) and the (110) models affects the shape of profiles of the partial density of segments. Figure 15 presents the density profiles for the fractions of f- and t-chains $\rho(x|y)$ with the free ends fixed at the layer y (inside or outside the LC layer in the MSB state). Due to stretching of polymer chains in the conventional brush (see refs 6−11), $\rho_{CB}(x|y)$ has a sharp peak at the point $x \sim y$ and quickly goes to zero at $x > y$:

$$\rho_{CB}(x|y) \sim \begin{cases} \dfrac{1}{\sqrt{y^2-x^2}}, & x < y \\ 0, & x > y \end{cases} \qquad N \to \infty \qquad (22)$$

The shape of $\rho(x|y)$ for f-chains in the (111) model as well as the behavior of t-chains in both (111) and (110) models is qualitatively similar to $\rho_{CB}(x|y)$. The behavior of $\rho(x|y)$ for f-chains in the (110) model is completely different: it is a boxlike profile of width equal to l_t. This means that the (110) polymer chains in the LC layer are not stretched at all and are folded to fill the LC layer.

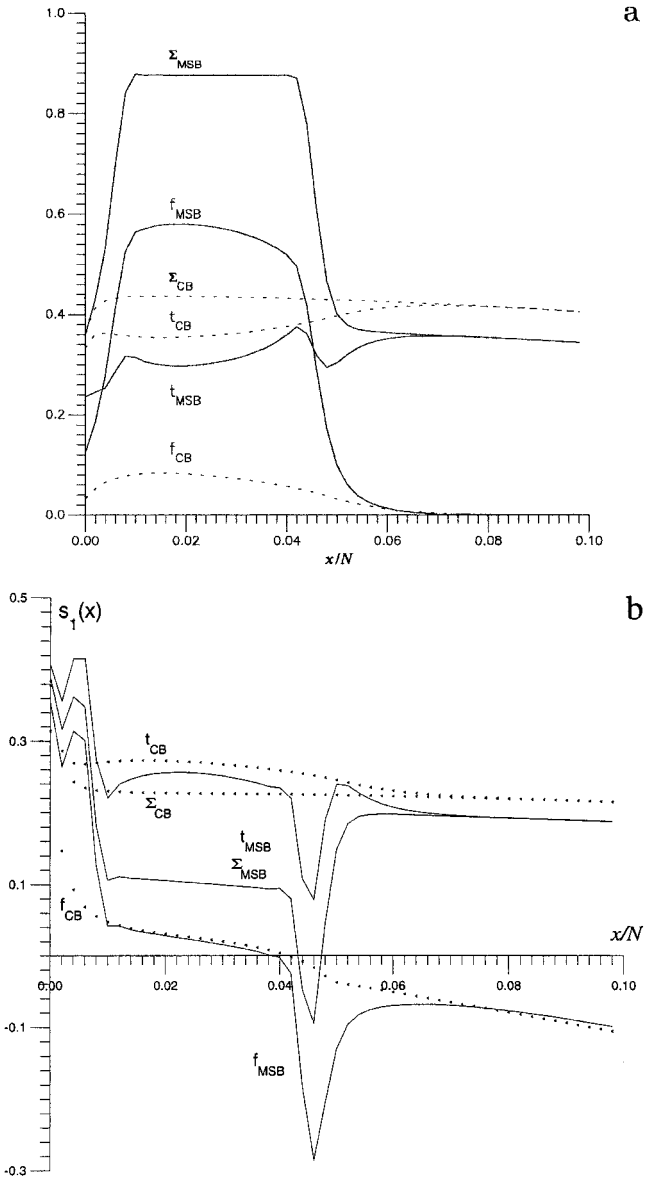

Figure 14. Partial densities $\rho(x)$ (a) and degrees of stretching $s_1(x)$ (b) of CB (dots) and MSB (solid lines) brushes in the transition point $\eta \simeq \eta_t$ versus x/N. Summary, f-chain, and t-chain data marked by symbols Σ, f, and t, correspondingly. $\sigma = 0.10$; $\chi = 0.25$; $N = 500$; $\eta = 3$; $l_t/N \simeq 0.05$; 6-choice SCL.

A more detailed investigation of various partial characteristics will be presented elsewhere.

3.6. Conclusions and Further Problems. In this paper we have investigated theoretically the LC ordering in polymer brushes formed by macromolecules with mesogenic groups in the main chain and immersed in a solvent.

Two phenomena related to the phase nature of this order−disorder transition are found:

- The existence of the MSB regime in which the brush is phase segregated into two sublayers. The intrinsic sublayer shows up as a collapsed orientationally ordered LCB brush. It is separated from the external swollen CB sublayer by an interphase boundary.
- At the transition point, this microphase-segregated state of the brush emerges discontinuously in the case

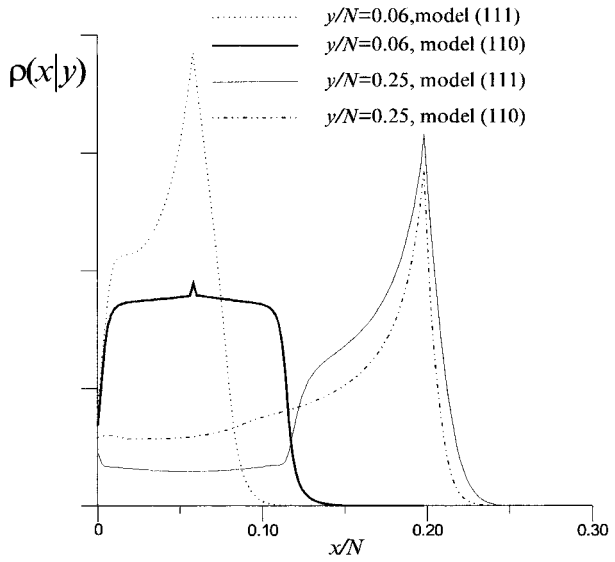

Figure 15. Profiles of partial density of segments $\rho(x|y)$ of the chains with the free ends fixed at the layer y (numbers on the curves): $\sigma = 0.10$; $\chi = 0.25$; $N = 500$, $h_{lc}/N - 0.12$; $\eta = 3$ (model (111)) and $\eta = 4$ (model (110)).

of the finite length N of grafted chains. In the $N \rightarrow \infty$ limit, the transition looks like a continuous second-order phase transition which is the result of the first-order phase transition taking place in an infinitesimally small part of the system. The phase nature of this transition is established provided the grafting density σ in the brush is not too large.

These results show that the inhomogeneity of the brush (in normal direction) is enhanced markedly when passing from a conventional brush (CB) to a brush undergoing an orientational ordering due to interactions between mesogenic groups. It is evident that theoretically one can get microphase separation inside the brush only when using a model that allows for the possible inhomogeneity of the system. The boxlike model does not satisfy this condition. As a result, it predicts liquid-crystalline ordering to be a first-order jumpwise transition in a brush as a whole.[15] Here, the boxlike model of the brush and our more detailed SCF model provide the results that differ not only quantitatively (as usual) but also qualitatively.

Nevertheless, the conclusions obtained for the boxlike model[15] in spite of their being an artifact of the model are very helpful in giving an insight into the present data. Let us return to Figure 3. In the CB state at small energy η of the anisotropic interactions the brush is characterized by the density profile changing from the maximum value $\rho = \rho_{max}$ at small x/N to $\rho = 0$ at large x/N (Figures 1a and 2a). Let us fix the point $\rho = \rho_{max}$ on the y-axis of Figure 3 and move parallel to the x-axis. Providing ρ_{max} is smaller than ρ_{crit}, at a certain value of η we encounter the lower branch of the binodal for the boxlike model. At this value of η the homogeneous brush should go to the liquid-crystalline state. For our inhomogeneous brush this value of η is sufficient to produce a transition only in the denser inner part of the brush. This part (the internal sublayer) cannot be too thin to avoid a strong contraction of chains confined in this sublayer. It cannot be too thick at the transition point in order to avoid the strong supercooling of the dense part of the layer in the disordered state. As follows from the present results for flexible 6-choice SCL chains grafted not too densely ($\sigma < 0.2$), the initial thickness of this sublayer scales as $N^{1/2}$. The other less dense part of a layer (external sublayer) formed by the tails of the chains traveling through the LC sublayer retains the disordered structure.

At the point of transition η_t the fraction of segments in the ordered sublayer scales as $N^{-1/2}$. The characteristics of this sublayer as functions of η exhibit a jump. Averaged over the whole brush, it is detectable only if N is finite, because $N^{-1/2}$ tends to zero as $N \rightarrow \infty$. In the $N \rightarrow \infty$ limit, the transition in an inhomogeneous brush resembles a continuous second-order phase transition which is a result of the first-order phase transition taking place in an infinitesimally small part of the system. Note that the transition in an inhomogeneous system does not have to be equivalent to the conventional phase transition in a homogeneous system. This problem needs additional study.

The other problem is related to the dependence of η_t and the sublayer width l_t on N at the transition point. There are several mechanisms which may account for these dependences: the loss of free energy at the interface boundary inside the layer, the contraction of chains confined inside the intrinsic sublayer, the difference in the mean density of sublayers undergoing the transition. Note that in any case it does not seem to be easy to reconcile two scaling dependences $\Delta\eta_t \approx N^{-1}$ and $l_t \sim N^{\alpha}$ with $\alpha = {}^1/_2$. However, these dependences were investigated only for the case of flexible chains. We are planning to present a more detailed analysis elsewhere.

Acknowledgment. We acknowledge the International Science Foundation, Russian Government (Grants NT 8000 and NT 8300) and the Russian Foundation for Basic Research (Grant 96-03-33862) for financial support. The authors express their gratitude to L. I. Klushin for discussion.

References and Notes

(1) Alexander, S. *J. Phys. (Paris)* **1977**, *38*, 977.
(2) DeGennes, P.-G. *Macromolecules* **1980**, *13*, 1069.
(3) Birshtein, T. M.; Zhulina, E. B. *Polymer* **1994**, *25*, 1453.
(4) Scheutjens, J. M.; Fleer, G. J. *J. Phys. Chem.* **1979**, *83*, 1619.
(5) Semenov, A. N. *Sov. Phys. JETP* **1985**, *61*, 733.
(6) Zhulina, E. B.; Pryamitsyn, V. A.; Borisov, O. V. *Polym. Sci. USSR* **1989**, *30*, 205.
(7) Milner, S. T.; Witten, T. A.; Cates, M. E. *Macromolecules* **1988**, *21*, 2610.
(8) Zhulina, E. B.; Borisov, O. V.; Pryamitsyn, V. A.; Birshtein, T. M. *Macromolecules* **1991**, *24*, 140.
(9) Amoskov, V. M.; Pryamitsyn, V. A. *Faraday Trans.* **1994**, *90* (6), 889.
(10) Amoskov, V. M.; Pryamitsyn, V. A. *Polym. Sci.* **1995**, *A37*, N7.
(11) Milner, S. T. *Science* **1991**, *251*, 905.
(12) Pickett, G. T.; Witten, T. A. *Macromolecules* **1992**, *25*, 4569.
(13) Kolegov, B. I. Thesis Inst. Macromol. Compounds, Leningrad, USSR, 1983.
(14) Wijmans, C. M.; Leermakers, F. A. M.; Fleer, G. J. *J. Chem. Phys.* **1994**, *101*, 8214.
(15) Mercurieva, A. A.; Birshtein, T. M.; Pryamitsyn, V. A.; Polotskij, A. *Macromol. Chem., Theory Simul.* **1996**, *5*, 215.
(16) Flory, P. J. *Principles of Polymer Chemistry*; Cornell University Press: New York, 1953.
(17) DeGennes, P.-G. *Scaling Concepts in Polymer Physics*; Cornell University Press: Ithaca, NY, 1979.

MA9603140